Seasonal changes in zooplankton abundance, biomass, size structure and dominant copepods in the Oyashio region analysed by an optical plankton counter

Atsushi Yamaguchi*, Kohei Matsuno, Yoshiyuki Abe, Daichi Arima and Kohei Ohgi

Laboratory of Marine Biology, Graduate School of Fisheries Sciences, Hokkaido University, 3-1-1 Minatomachi, Hakodate, Hokkaido, 041-8611 Japan

*: Corresponding author: Tel: +81 138 40 5543, Fax: +81 138 40 5542.
E-mail address: a-yama@fish.hokudai.ac.jp (A. Yamaguchi).

Abstract

To identify seasonal patterns of change in zooplankton communities, an optical plankton counter (OPC) and microscopic analysis were utilised to characterise zooplankton samples collected from 0 to 150 m and 0 to 500 m in the Oyashio region every one to three months from 2002 to 2007. Based on the OPC measurements, the abundance and biomass of zooplankton peaked in June (0-150 m) or August (150-500 m), depending on the depth stratum. The peak periods of the copepod species that were dominant in terms of abundance and biomass indicated species-specific patterns. Three *Neocalanus* species (*N. cristatus, N. flemingeri* and *N. plumchrus*) exhibited abundance peaks that occurred before their biomass peaks, whereas *Eucalanus bungii* and *Metridia pacifica* experienced biomass peaks before their abundance peaks. The abundance peaks corresponded to the recruitment periods of early copepodid stages, whereas the biomass peaks corresponded to the periods when the dominant populations reached the late copepodid stages (C5 or C6). Because the reproduction of *Neocalanus* spp. occurred in the deep layer (>500 m), their biomass peaks were observed when the major populations reached stage C5 after the abundance peaks of the early copepodid stages. The reproduction of *E. bungii* and *M. pacifica* occurred near the surface layer. These species first formed biomass peaks of C6 and later developed abundance peaks of newly recruited early copepodid stages. From the comparison between OPC measurements and microscopic analyses, seasonal changes in zooplankton biomass at depths of 0 to 150 m were governed primarily by *E. bungii* and *M. pacifica*, whereas those at depths of 150 to 500 m were primarily caused by the three *Neocalanus* species.

Keywords: *Eucalanus*, *Metridia*, *Neocalanus*, ESD, life cycle, OPC

1. Introduction

The Oyashio region is located in the western subarctic Pacific and is influenced by the Oyashio Current, which mixes with the colder, less saline water of the Okhotsk Sea on its way southwest from the Kurile Islands (Kono, 1997). The Oyashio region is sometimes covered with warm-core rings from the Kuroshio Current (Yasuda et al., 1992; Kono, 1997). Seasonal changes in the Oyashio pelagic ecosystem are characterised by a massive phytoplankton bloom in spring and a subsequent increase in zooplankton biomass (Kasai et al., 1997, 2001; Saito et al., 2002). The zooplankton biomass in this region is dominated by large grazing copepods (*Neocalanus* spp., *E. bungii* and *M. pacifica*) (73% of total zooplankton biomass, cf. Ikeda et al., 2008). Information on the life cycle patterns of these copepods has accumulated rapidly during the past decade (Kobari and Ikeda, 1999, 2001a, 2001b; Tsuda et al., 1999, 2004). However, information on whole zooplankton communities, especially seasonal changes in their sizes, is scarce.

From the viewpoint of fisheries, the prey size of pelagic fishes is known to vary with ontogeny (Oozeki et al., 2004). Information on zooplankton size composition is important because it affects fish energy costs and growth and mortality rates (van der Meeren and Næss, 1993; Yamamura, 2004) and regulates the vertical particulate flux through the biological pump (Boyd and Newton, 1999; Ducklow et al., 2001). Little information is available on the size composition of zooplankton in the Oyashio region. This is partly because evaluating size for zooplankton samples via ordinary microscopic analysis is very time-consuming. To overcome this problem, analysis of zooplankton samples using an Optical Plankton Counter (OPC) (Herman, 1988, 1992; Beaulieu et al., 1999) can provide accurate sizes and numbers of zooplankton much more quickly than

55 microscopic analysis.

56 In this study, we performed an OPC analysis on preserved zooplankton samples
57 collected from 0-150 m and 0-500 m in the Oyashio region every one to three months
58 from 2002-2007 (six years). Large grazing copepod species (*Neocalanus* spp., *E.*
59 *bungii* and *M. pacifica*) were identified, classified by stage, and counted. Based on
60 these copepod data, we also evaluated the seasonal pattern of change in the species
61 composition of the dominant copepods within the 0-500 m stratum of the Oyashio
62 region. Finally, knowing the size of each copepodid stage, we were able to estimate
63 the copepod species composition of the zooplankton biomass based on its size
64 distribution, and we determined which species govern seasonal changes in the
65 zooplankton biomass within the Oyashio region.

66 **2. Material and Methods**

67 *2.1. Zooplankton sampling*

68 Zooplankton samples were collected with twin NORPAC nets (0.335 mm and
69 0.100 mm mesh, Motoda, 1957) at Site H (41˚30'N, 145˚47'E, Fig. 1) in the Oyashio
70 region of the western subarctic Pacific every one to three months from May 2002 to
71 December 2007. The total number of samples was 56 (Table 1). The twin NORPAC
72 nets were equipped with a flow-meter (Rigosha Co. Ltd.) in their mouths to register the
73 volume of water filtered. The filtration efficiency of the net was 99.4±2.2% (mean±1
74 sd) for the 0.335 mm mesh and 90.7±3.6% for the 0.100 mm mesh. Because both nets
75 had the same mouth diameter, some of the larger animals may have been excluded by
76 both nets in this study. Samples were preserved on board in 5% borax-buffered
77 formalin in seawater. Temperature and salinity data were obtained with a CTD system

78 (Sea-Bird SBE-911 Plus).

79

80 *2.2. OPC measurement*

81 For optical analysis, a laboratory OPC (Model OPC-1 L, Focal Technologies
82 Inc.) with a 2 x 2 cm opening and a 4-mm-thick beam, developed to sense zooplankton
83 flow through the system (Herman, 1988), was utilised in this study. To measure the
84 sizes of the dominant copepods, we performed an OPC analysis on 30 individuals of
85 each copepodid stage of *N. cristatus, N. flemingeri, N. plumchrus, E. bungii* and *M.*
86 *pacifica* sorted from the formalin-preserved samples collected in the Oyashio region.
87 The prosome length (PL) of each copepodid stage was also measured under a dissecting
88 microscope to the nearest 0.03-0.10 mm, depending on the stage.

89 OPC measurements were made on samples collected by a 0.335-mm mesh size
90 twin NORPAC net (0-150 m and 0-500 m) (Table 1). Zooplankton samples were split
91 (Motoda, 1959), and half of the aliquots were filtered on 0.100-mm mesh under low
92 vacuum and then weighed (wet mass: WM) to a precision of 0.01 g (Mettler PM4000).
93 Subsamples (1/2–1/16) of the remaining aliquots were used for OPC measurements.
94 Procedures for OPC measurements followed those of Yokoi et al. (2008); thus, (1) the
95 flow rate of samples was approximately 10 L $min.^{-1}$, (2) zooplankton counts were kept
96 to less than 10 counts $sec.^{-1}$ and (3) counts were performed once without staining to
97 avoid damage to the specimens. This flow rate is substantially lower than that of
98 another other study using the same laboratory OPC-1 L (25 L $min.^{-1}$, Moore and Suthers,
99 2006).

100 *2.3. Microscopic analysis*

In the Oyashio region, large copepods (*N. cristatus, N. flemingeri, N. plumchrus, E. bungii and M. pacifica*) are known to dominate the mesozooplankton biomass (73% of annual mean, Ikeda et al., 2008). To evaluate growth across the whole population, we examined samples from 0–500 m collected with 0.100-mm mesh. For collection efficiency between the 0.335 mm and 0.100 mm mesh nets, stages C1-C6 of *E. bungii* and *Neocalanus* spp. were all quantitatively collected by both nets, whereas C1-C3 of *M. pacifica* were not quantitatively collected with the 0.335 mm mesh (Yamaguchi et al., 2010). We counted each copepodid stage of the five species listed above based on subsamples (1/1–1/40, made with a wide-bore pipette). We multiplied the individual dry mass of each stage (Ueda et al., 2008) by the abundance of that stage counted in each sample.

2.4. OPC data processing

2.4.1. Abundance

Based on the OPC data, the zooplankton abundance was calculated within each of 4096 equivalent spherical diameters (ESD, mm) as follows:

$$N = \frac{n}{s \times F} \quad (1)$$

where N is abundance (N: ind. m^{-3}), n is counted number, s is the subsample factor and F is the volume of water filtered through net towing (m^3). From the abundance data (N), we calculated standing stocks (ind. m^{-2}, 0-150 or 0-500 m) by multiplying by the maximum depth (150 or 500 m).

2.4.2. Biomass

Based on OPC-derived ESD data (mm), the biovolume (mm^3) of zooplankton within each 4,096 ESD size unit was calculated (i.e., biovolume = $4/3\pi[ESD/2]^3$). The wet mass (mg WM) of each size class was calculated from the biovolume of a size-specific particle, assuming the specific gravity of zooplankton to be equal to that of water (e.g., 1 mg WM = 1 mm^3). Assuming the water content of zooplankton to be 90% (cf. Yamaguchi et al., 2005), DM was calculated (DM = 0.1 x WM). Thus, the obtained DM conversion factor of each 4,096 ESD size unit (g DM $ind.^{-1}$) was multiplied by the abundance (ind. m^{-3} or ind. m^{-2}) to obtain the total DM (g DM m^{-3} or g DM m^{-2}).

2.5. Analysis of seasonal sequence

We constructed seasonal changes for each parameter based on data from multiple years (cf. Miller and Terazaki, 1989; Osgood and Frost, 1994). The procedures used were based on those of Osgood and Frost (1994), who evaluated the life cycles of three copepods in Dabob Bay, Washington based on assemblage data that were constructed from data from multiple years (1973, 1982 and 1983).

Integrated mean temperature and salinity in the 0-150 m depth stratum were calculated for each sampling date. The data were arranged in order of Julian day (365 days) without reference to year. Data between the sampling dates were linearly interpolated at intervals of 15 days. For each parameter, data were smoothed by applying a 30-day moving average.

The abundance and biomass estimates derived from the OPC analysis were summed into six ESD size classes (<0.5, 0.5-1.0, 1.0-2.0, 2.0-3.0, 3.0-4.0 and >4.0 mm). For each size class, a seasonal time series was obtained via the same method applied to

145 the environmental parameters. The abundance and biomass in ind. m^{-2} and g DM m^{-2},
146 respectively, in the 150-500 m stratum were calculated by subtracting the 0-150 m
147 values from the 0-500 m values. This depth-subtraction step, called the "subtracting
148 method", has not been used recently; however, this method of estimating the abundance
149 of zooplankton in a discrete depth interval (without the use of an opening/closing net)
150 was used >50 years ago (Motoda and Anraku, 1954, 1955). For the abundance and
151 biomass of large copepods obtained by microscopic analysis, data were standardised
152 with the procedures mentioned above.

153 **3. Results**

154 *3.1. OPC calibration and dominant copepods*

155 There was a highly significant correlation between the OPC-derived ESD (Y)
156 and PL (X) of copepods: $Y = 0.478\ X$ ($r^2 = 0.96$, $p < 0.0001$, Fig. 2a). For total WM,
157 there was a highly significant correlation between OPC-derived WM (Y') and directly
158 measured WM (X'): $Y' = 0.934X'$ ($r^2 = 0.67$, $p < 0.0001$). Because the conversion
159 factor (0.934) was slightly lower than 1, the OPC measurement slightly underestimated
160 the directly measured values (Fig. 2b). The ESD size classes of each copepodid stage
161 of dominant copepod species are shown in Table 2. Based on our six composite ESD
162 size classes (<0.5, 0.5-1.0, 1-2, 2-3, 3-4 and >4.0 mm), the copepodid ESD sizes of the
163 dominant copepod species were <0.5, 0.5-1.0, 1-2, 2-3 and 3-4 mm. Because the
164 ESDs of dominant copepods were smaller than 4.0 mm, the size class >4.0 mm was
165 thought to consist of the large zooplankton (e.g., chaetognaths, salps and euphausiids).

166 *3.2. Seasonal changes in hydrography*

167 The integrated temperature in the 0-150 m stratum of the water column varied
168 between 2.9˚C in March and 11.0˚C in November (Fig. 3a). The temperature peaked
169 in November, decreased until March, gradually increased until September, and then
170 rapidly increased from September to November. The integrated mean salinity in the
171 0-150 m stratum varied between 33.16 in September and 33.75 in November. The
172 high-salinity season (November) corresponded to the peak temperature (Fig. 3a). In
173 terms of the water masses, the low-temperature and less saline Oyashio water
174 dominated from January to September, whereas the higher-temperature and saline water
175 was observed in November; a mixture of these two waters was observed in October and
176 December (Fig. 3b).

177 *3.3. Seasonal changes in zooplankton (OPC analysis)*

178 The zooplankton abundance peaked in June in the 0-150 m stratum and in
179 August for the deeper stratum (150-500 m) (Figs. 4a, b). The abundance peak at 0-150
180 m was 138,000 ind. m^{-2}, and the <0.5-mm and 0.5-1.0-mm size classes predominated
181 (ca. 80% of total zooplankton, Fig. 4a). The abundance peak at 150-500 m was lower
182 (105,000 ind. m^{-2}) than that for 0-150 m (Fig. 4b). The contribution to abundance
183 from the <0.5-mm size class was lower than those of the 0.5-1.0-mm and 1.0-2.0-mm
184 size classes for the 150-500 m stratum.

185 Zooplankton biomass also peaked in June for the shallower stratum (0-150 m,
186 10.7 g DM m^{-2}) and in August for the deeper stratum (150-500 m, 14.4 g DM m^{-2}) (Fig.
187 4c, d). These biomass peak seasons corresponded to the peaks in abundance. The
188 peak biomass values for the 150-500 m stratum were greater than those for 0-150 m.
189 This depth pattern of biomass was opposed to that of abundance. For biomass, the

190 contribution of the smaller size classes was smaller than that of larger ones.

191 The seasonal changes in biomass of each size class at each depth are shown in
192 Fig. 5. The peak in total biomass at 0-150 m was in June (Fig. 4c), and the size classes
193 that peaked in the same period were <0.5, 1.0-2.0 and 2.0-3.0 mm (Figs. 5a, c, d). For
194 the 150-500 m stratum, the total biomass peaked in August (Fig. 4d), and the size
195 classes of 0.5-1.0, 2.0-3.0, 3.0-4.0 and >4.0 mm had peaks in that period (Figs. 5b, d, e,
196 f). Based on their dominant contributions to biomass and similar seasonal patterns, the
197 seasonal sequences of both depth strata were driven primarily by the size classes of
198 1.0-2.0 and 2.0-3.0 mm.

199 *3.4. Seasonal changes in dominant copepods (microscopic analysis)*

200 The seasonal changes in abundance and biomass, as well as the corresponding
201 stage compositions of dominant copepod species at 0-500 m, are shown in Figs. 6 and 7.
202 The abundance of *Neocalanus cristatus* was greater in February (6,680 ind. m^{-2}) and
203 lower from July to November (ca. 1,500 ind. m^{-2}, Fig. 6a). The abundance of *N.*
204 *cristatus* C1 peaked from December - January (64%), developed through C2-C4, and
205 then reached C5 between April and July. The mean biomass of *N. cristatus* was
206 greater from April to August (1.2-1.9 g DM m^{-2}), and C5 predominated in biomass
207 throughout the year. C6 individuals were very rare above 500 m.

208 The abundance of *Neocalanus flemingeri* peaked at 8,566 ind. m^{-2} in March,
209 and dropped to scarcity (approximately 900 ind. m^{-2}) from July to December (Fig. 6b).
210 Early copepodid stages predominated in March (C1-C3 comprised 66% of total). This
211 population developed to C5 in June and C6 in July. The biomass of *N. flemingeri*
212 exhibited a sharp peak from May-June (1.5 g DM m^{-2}), and C5 and C6 dominated the

biomass at that period (80-100%). During January to April, the composition of C4 was also high (ca. 40%).

The maximum abundance of *Neocalanus plumchrus* reached 12,349 ind. m^{-2} from April to July, and the abundance of stage C1 peaked in May (Fig. 6c). This newly recruited population developed through C2 to C4, reaching C5 in July. The biomass of *N. plumchrus* reached a sharp peak in July, and C4 and C5 were the predominant stages, while their dominant period varied seasonally: December to March for C4 and May to October for C5.

The abundance of *Eucalanus bungii* varied from 2,746 to 26,929 ind. m^{-2} and was greatest from June to August (Fig. 7a). C1 and C2 were only observed from April to August, whereas C3-C6 predominated during the rest of the year. The abundance of C6 was highest in February for males and in April for females, which was one to two months earlier than the peak of C1 abundance. The biomass peak of *E. bungii* was 3.0 g DM m^{-2} in May, earlier than the peak for abundance (June to August). Late copepodid stages such as C5 and C6 were the major component of the *E. bungii* biomass.

The abundance of *Metridia pacifica* varied from 10,180 ind. m^{-2} in February to 54,056 ind. m^{-2} in June and was highest from May to July (Fig. 7b). Early copepodid stages such as C1-C3 were abundant from May to July. The biomass of *M. pacifica* peaked in April (2.9 g DM m^{-2}) and was composed primarily of C6, whereas the ratio of C5 to C6 increased in June-August.

4. Discussion

4.1. OPC calibration

There are several possibilities for under- or overestimation of sizes or numbers of particles by the OPC. Contributions from detritus and large phytoplankton to OPC data are inevitable for *in-situ* OPC (OPC-2T). However, for laboratory use of an OPC (OPC-1 L) as in this study, those factors (detritus and large phytoplankton) were eliminated by excluding samples dominated by detritus and large phytoplankton from the analyses (cf. Moore and Suthers, 2006). Underestimation of numbers can be caused by coincidences of particles, and underestimation of size can occur as a result of the transparent bodies of some zooplankters (Herman, 1992; Sprules et al., 1998; Zhang et al., 2000). Overestimation of body sizes can be caused by coincidences of particles, and overestimation of numbers can be caused by the presence of detritus and fragments of damaged specimens (Sprules et al., 1998; Beaulieu et al., 1999; Zhang et al., 2000). For the measurement of preserved samples, shrinkage of body sizes in gelatinous zooplankton causing underestimation of sizes and reduction of body transparency in copepods causing overestimation of sizes have been reported as sources of error in OPC measurements (Beaulieu et al., 1999).

In the present study, samples were omitted if phytoplankton or large salps dominated the biomass (8 of 112 samples were excluded, see plot in Fig. 2b). If we include these data, the factor changes greatly ($Y' = 0.934\ X'$ to $Y' = 0.438\ X'$). Samples where phytoplankton predominated had low biomass estimates from the OPC measurements. Because the OPC could only detect particles larger than 250 μm ESD, it may not adequately measure phytoplankton-dominated samples. Furthermore, the degree of underestimation is known to be large for sizes near the instrument detection limits (Herman, 1992).

A significant positive correlation was observed between OPC-derived ESD

and the PL of copepods (Fig. 2a). Huntley et al. (2006) reported the relationship between copepod PL and OPC ESD off Hawaiian waters to be $PL = 1.9 \times ESD$. Although the location (subarctic vs. subtropical) and target species vary between that study and the present work, our obtained equation, $PL = 2.0 \times ESD$ (i.e., $ESD = 0.478 \times PL$, Fig. 2a), is very similar to that of Huntley et al. (2006). This suggests that differences in copepod species composition have little effect on the relationship between the ESD and PL of copepods.

4.2. Hydrography

The integrated mean temperature and salinity of the 0-150 m depth range in the Oyashio region varied with season (Fig. 3a). According to the classification of water masses by Hanawa and Mitsudera (1987), the water mass in November was the Tsugaru Warm Water (Fig. 3b). Hanawa and Mitsudera (1987) also noted that the mixture of Kuroshio and Oyashio water may plot within the Tsugaru Warm Water in their T-S diagram. Yasuda et al. (1992) reported that warm-core rings separated from Kuroshio often move northwards to 40˚N latitudes. Bearing this in mind, we considered that the water mass in November classified as the Tsugaru Warm Water in this study might also be a mixture of Kuroshio and Oyashio waters. Per the hydrographic characteristics of the Oyashio region, the variability in T-S diagrams from January to September was lower than that from October to December. Thus, the water mass at the 0-150 m depth range within the Oyashio region was separated into two seasons: January-September, when the water is dominated by the local Oyashio water, and October-December, when the water is dominated by the mixture of Kuroshio and Oyashio waters.

4.3. Life cycle of copepods

The seasonal developmental pattern estimated by tracing the sequence of mean copepodid stages of the population at each sampling date revealed that the recruitment season of the C1 population was January for *N. cristatus*, March for *N. flemingeri* and May for *N. plumchrus* and *E. bungii*. In contrast to these copepods with single recruitment seasons per year, *M. pacifica* exhibited continuous recruitment. The phenology of reproduction and development for these copepods reflects species-specific differences in their energy utilisation patterns; *M. pacifica* and *E. bungii* spawn in the phytoplankton-rich surface layer in spring (females need to feed for spawning), whereas *Neocalanus* spp. spawn in deeper water in winter (females do not feed). The development from C1 to C5 of *N. cristatus*, *N. flemingeri* and *N. plumchrus* occurs from January to June, March to June and May to August, respectively; thus, the three sympatric *Neocalanus* spp. exhibited a clear temporal separation in their developmental timing in the western subarctic Pacific. This temporal separation in utilising the surface layer is considered to be a mechanism to reduce inter-specific food competition.

The copepod abundance peaks measured here all corresponded with the peak period of recruitment of the early copepodid stage of each species. Their biomass peaks corresponded with the seasons when the majority of each population reached the late copepodid stages (Figs. 6, 7). Interestingly, the order of the abundance and biomass peaks varied with species. For *Neocalanus* spp., the biomass peaks were observed after the abundance peaks. In contrast, the biomass peaks of *E. bungii* and *M. pacifica* were observed well before the abundance peaks. The species-specific

differences in the sequence of the abundance and biomass peaks are attributed to their ontogenetic vertical migrations and our maximum sampling depth. *Neocalanus* spp. are known to develop to C5 at the surface layer, then migrate down to deep layers, where they develop to C6 and reproduce without feeding. Because of this life-cycle schema, it is reasonable that their biomass peaks are observed when they reach C5, after the abundance peak (recruitment of juvenile stages) at the surface layer (Fig. 6). In contrast to *Neocalanus* spp., reproduction in *E. bungii* and *M. pacifica* is performed by overwintered specimens at the surface layer, and their biomass peaks thus correspond to the peak of C6F, which occurs earlier than the abundance peaks (composed of the subsequent juvenile stages) (Fig. 7). Hence, the species-specific differences in the sequence of the abundance and biomass peaks are based on species' life-cycle patterns, the study's maximum sampling depth, and our seasonal reference (January to December).

4.4. Seasonal changes in zooplankton size composition

To clarify which species had the greatest influences on the seasonal changes in the biomass of each size class, we combined stage-specific size-class data (Table 2) with seasonal changes in stage-specific biomass data for the 0-500 m depth range (Figs. 6 and 7) and then added the seasonal biomass data for 0-500 m derived from OPC (Fig. 8). In this calculation, the remaining fraction is regarded as "Others" (Fig. 8). Differences in mesh size between the OPC (0.335 mm) and microscopic (0.100 mm) analyses had little effect on the results in terms of biomass. All of the copepodid stages (C1-C6) of *Neocalanus* spp. and *E. bungii* were quantitatively collected by both nets, whereas C1-C3 of *M. pacifica* were not quantitatively collected by the 0.335 mm

329 mesh (Yamaguchi et al., 2010). However, the copepod biomass was dominated by the
330 middle to late copepodid stages (cf. Figs. 6 and 7), i.e., those stages that were
331 quantitatively collected with both mesh sizes. We applied only biomass units to
332 combine the OPC and microscopic data. Thus, we see little effect of the difference in
333 mesh size on the biomass analysis.

334 The size classes of the late copepodid stages of *Eucalanus bungii* and
335 *Metridia pacifica*, which reproduce in the surface stratum, were 1.0-2.0 and 2.0-3.0 mm
336 (Table 2, Figs. 8c, d). The late copepodid stages of *Neocalanus* spp. were primarily
337 composed of the size classes of 2.0-3.0 and 3.0-4.0 mm (Table 2, Figs. 8d, e). The
338 biomass peak of 1.0-2.0 mm in the 0-150 m stratum was observed from May to June
339 (Fig. 5c), corresponding to the period when *M. pacifica* dominated (Fig. 8c). The
340 biomass peak of 2.0-3.0 mm at 0-150 m was in May (Fig. 5d), corresponding to the
341 period when *E. bungii* dominated (Fig. 8d). For the 150-500 m stratum, a clear peak
342 was observed in the size class of 2.0-3.0 mm in August (Fig. 5d), corresponding to the
343 period when *N. plumchrus* dominated (Fig. 8d). From these results, it could be
344 inferred that the biomass peak at 0-150 m was caused primarily by the two
345 surface-spawners, *E. bungii* and *M. pacifica*, whereas the biomass peak at 150-500 m
346 was governed mainly by the larger *Neocalanus* spp. Thus, the depth-related
347 differences in seasonal changes in zooplankton biomass are due to the depth strata being
348 governed by different species: *E. bungii* and *M. pacifica* for 0-150 m and *Neocalanus*
349 spp. for 150-500 m.

350 The annual mean ratio of these dominant copepods to the total zooplankton in
351 terms of biomass was approximately 48% (Fig. 8f). This composition ratio is lower than
352 the 73% reported for the zooplankton biomass in the water column from 0-2,000 m

353 (Ikeda et al., 2008). Because our estimation covers only 0-500 m, it appears to omit
354 most of the diapausing *Neocalanus* fraction, which is known to sink below 500 m
355 during its ontogenetic vertical migration (Kobari and Ikeda, 1999, 2001a, 2001b). The
356 body size of pre-adult *Neocalanus* spp. stages during diapausing is large, so their
357 contribution to the total zooplankton biomass may increase at depths greater than 500 m.
358 For example, export flux by ontogenetic vertical migration of *Neocalanus* spp. is
359 estimated to be approximately 92% of sinking passive carbon flux at 1,000 m in the
360 Oyashio region (Kobari et al., 2003). From other studies in the subarctic Pacific, the
361 active particle organic carbon (POC) flux by ontogenetic vertical migrating *Neocalanus*
362 spp. is known to be greater than the passive POC (Kobari et al., 2008).

363 For the smallest size class (<0.5 mm), there was one period when the
364 microscopically estimated biomass was greater than the biomass estimated by OPC
365 (March to July, Fig. 8a). This is partly caused by the difference in mesh sizes, which
366 were 0.100 mm for the microscopic analysis and 0.335 mm for the OPC. Furthermore,
367 we should consider that the OPC can only detect particles greater than 0.25 mm ESD.
368 Because the diagonal length of 0.335 mm mesh is 0.474 mm, OPC analysis may not
369 quantitatively evaluate the <0.5-mm size class. Nevertheless, the "Others" dominated
370 the biomass in the <0.5-mm size class from October to December (Fig. 8a). This
371 period (October to December) corresponded to the period when warm-core rings
372 frequently separate from the Kuroshio Current (Fig. 3b). During October to December,
373 the total biomass of the <0.5-mm size class remained high, whereas the abundance of *M.*
374 *pacifica* exhibited a sudden decrease. In the Oyashio region, small warm-water
375 oncaeid copepods dominate the zooplankton community of warm-core rings (Nishibe
376 and Ikeda, 2004). Thus, the dominance of "Others" in the <0.5-mm size class during

October to December might be particularly affected by a warm-core ring that separated from the Kuroshio Current.

In conclusion, the method of this study—combining OPC analysis and microscopic analysis on the same samples—is valuable. From these analyses, we can obtain both size and taxonomic information. Applying the individual size and biomass data for each copepodid stage, the composition of each size class of each species in the biomass was evaluated (Fig. 8). Such comprehensive insights into the size and species composition of the zooplankton biomass could not be obtained without this method. Recently, mesozooplankton size data obtained by OPC analysis were used for Normalised Biomass Size Spectra (NBSS) analysis (Matsuno et al., 2012; Marcolin et al., 2013). However, to concentrate on size-taxonomic analysis, we did not apply NBSS analysis in this study. In the future, NBSS analysis of seasonal zooplankton samples may be needed in the Oyashio region.

Acknowledgments

Drs Jeffery M. Napp and Deborah K. Steinberg provided useful comments on the manuscript. We are grateful to the captain, officers, crew, cadets and scientists on board T/S *Oshoro-Maru* and R/V *Ushio-Maru* of Hokkaido University for their help in collecting zooplankton samples and hydrographical data. This study was supported by Grant-in-Aid for Scientific Research (A) 24248032 and Grant-in-Aid for Scientific Research on Innovative Areas 24110005 from the Japan Society for the Promotion of Science (JSPS).

398 **References**

399 Beaulieu, S.E., Mullin, M.M., Tang, V.T., Pyne, S.M., King, A.L., Twining, B.S., 1999.
400 Using an optical plankton counter to determine the size distribution of
401 zooplankton samples. J. Plankton Res. 21 (10), 1939-1956.
402 Boyd, P.W., Newton, P.P., 1999. Does planktonic community structure determine
403 downward particulate organic carbon flux in different oceanic province? Deep-Sea
404 Res. I 46 (1), 63-91.
405 Ducklow, H.W., Steinberg, D.K., Buesseler, K.O., 2001. Upper ocean carbon export and
406 the biological pump. Oceanography 14 (4), 50-58.
407 Hanawa, K., Mitsudera, H., 1987. Variation of water system distribution in the Sanriku
408 coastal area. J. Oceanogr. Soc. Japan 42 (6), 435-446.
409 Herman, A.W., 1988. Simultaneous measurement of zooplankton and light attenuance
410 with a new optical plankton counter. Cont. Shelf Res. 8 (2), 205-221.
411 Herman, A.W., 1992. Design and calibration of a new optical plankton counter capable
412 of sizing small zooplankton. Deep-Sea Res. A 39 (3-4), 395-415.
413 Huntley, M.E., Lopez, M.D.G., Zhou, M., Landry, M.R., 2006. Seasonal dynamics and
414 ecosystem impact of mesozooplankton at station ALOHA based on optical
415 plankton counter measurements. J. Geophys. Res. C. 111 (C05S10),
416 doi:10.1029/2005JC002892.
417 Ikeda, T., Shiga, N., Yamaguchi, A., 2008. Structure, biomass distribution and
418 trophodynamics of the pelagic ecosystem in the Oyashio region, western subarctic
419 Pacific. J. Oceanogr. 64 (3), 339-354.
420 Kasai, H., Saito, H., Yoshimori, A., Taguchi, S., 1997. Variability in timing and
421 magnitude of spring bloom in the Oyashio region, the subarctic Pacific off

422 Hokkaido, Japan. Fish. Oceanogr. 6 (2), 118-129.
423 Kasai, H., Saito, H., Yoshimori, A., Kashiwai, M., Taneda, T., Kusaka, A., Kawasaki, Y.,
424 Kono, T., Taguchi, S., Tsuda, A., 2001. Seasonal and interannual variations in
425 nutrients and plankton in the Oyashio region: A summary of a 10 years
426 observation along the A-line. Bull. Hokkaido Natl. Fish. Res. Inst. 65, 57-136.
427 Kobari, T., Ikeda, T., 1999. Vertical distribution, population structure and life cycle of
428 *Neocalanus cristatus* (Copepoda: Calanoida) in the Oyashio region with notes on
429 its regional variations. Mar. Biol. 134 (4), 683-696.
430 Kobari, T., Ikeda, T., 2001a. Life cycle of *Neocalanus flemingeri* (Crustacea: Copepoda)
431 in the Oyashio region, western subarctic Pacific, with notes on its regional
432 variations. Mar. Ecol. Prog. Ser. 209, 243-255.
433 Kobari, T., Ikeda, T., 2001b. Ontogenetic Vertical migration and life cycle of
434 *Neocalanus plumchrus* (Copepoda: Calanoida) in the Oyashio region, with notes
435 on regional variations in body size. J. Plankton Res. 23 (3), 287-302.
436 Kobari, T., Shinada, A., Tsuda, A., 2003. Functional roles of interzonal migrating
437 mesozooplankton in the western subarctic pacific. Prog. Oceanogr. 57 (3-4),
438 279-298.
439 Kobari, T., Steinberg, D.K., Ueda, A., Tsuda, A., Silver, M.W., Kitamura, M., 2008.
440 Impacts of ontogenetically migrating copepods on downward carbon flux in the
441 western subarctic Pacific Ocean. Deep-Sea Res. II 55 (14-15), 1648-1660.
442 Kono, T., 1997. Modification of the Oyashio water in the Hokkaido and Tohoku area.
443 Deep-Sea Res. I 44 (4), 669-688.
444 Marcolin, C.R., Schultes, S., Jackson, G.A., Lopes, R.M., 2013. Plankton and seston
445 size spectra estimated by the LOPC and ZooScan in the Abrolhos Bank ecosystem

(SE Atlantic). Cont. Shelf Res. 70 (1), 74−87.

Matsuno, K., Yamaguchi, A., Imai, I., 2012. Biomass size spectra of mesozooplankton in the Chukchi Sea during the summers of 1991/1992 and 2007/2008: an analysis using optical plankton counter data. ICES J. Mar. Sci. 69 (7), 1205−1217.

Miller, C.B., Terazaki, M., 1989. The life histories of *Neocalanus flemingeri* and *Neocalanus plumchrus* in the Sea of Japan. Bull. Plankton Soc. Japan 36 (1), 27-41.

Moore, S.K., Suthers, I.M., 2006. Evaluation and correction of subresolved particles by the optical plankton counter in three Australian estuaries with pristine to highly modified catchments. J. Geophys. Res. C. 111 (C05S04), doi:10.1029/2005JC002920.

Motoda, S., 1957. North Pacific standard plankton net. Inform. Bull. Planktol. Japan 4, 13-15.

Motoda, S., 1959. Devices of simple plankton apparatus. Mem. Fac. Fish. Hokkaido Univ. 7 (1-2), 73-94.

Motoda, S., Anraku, M., 1954. Daily changes of vertical distribution of plankton animals near western entrance of the Tsugaru Strait, northern Japan. Bull. Fac. Fish. Hokkaido Univ. 5 (1), 15-19.

Motoda, S., Anraku, M., 1955. Further observation on the daily changes in amount of catches of plankton animals in vertical hauls. Bull. Fac. Fish. Hokkaido Univ. 6 (1), 15-18.

Nishibe, Y., Ikeda, T., 2004. Vertical distribution, abundance, and community structure of oncaeid copepods in the Oyashio region, western subarctic Pacific. Mar. Biol. 145 (5), 931-941.

Oozeki, Y., Watanabe, Y., Kitagawa, D., 2004. Environmental factors affecting larval growth of Pacific saury, *Cololabis saira*, in the northwestern Pacific Ocean. Fish. Oceanogr. 13 (S1), 44-53.

Osgood, K.E., Frost, B.W., 1994. Comparative life histories of three species of planktonic calanoid copepods in Dabob Bay, Washington. Mar. Biol. 118 (4), 627-636.

Saito, H., Tsuda, A., Kasai, H., 2002. Nutrient and plankton dynamics in the Oyashio region of the western subarctic Pacific Ocean. Deep-Sea Res. II 49 (24-25), 5463-5486.

Sprules, W.G., Herman, A.W., Stockwell, J.D., 1998. Calibration of an optical plankton counter for use in fresh water. Limnol. Oceanogr. 43 (3), 726-733.

Tsuda, A., Saito, H., Kasai, H., 1999. Life history of *Neocalanus flemingeri* and *Neocalanus plumchrus* (Copepoda: Calanoida) in the western subarctic Pacific. Mar. Biol. 135 (3), 533-544.

Tsuda, A., Saito, H., Kasai, H., 2004. Life history of *Eucalanus bungii* and *Neocalanus cristatus* (Copepoda: Calanoida) in the western subarctic Pacific Ocean. Fish. Oceanogr. 13 (S1), 10-20

Ueda, A., Kobari, T., Steinberg, D.K., 2008. Body length, weight and chemical composition of ontogenetically migrating copepods in the western subarctic gyre of the North Pacific Ocean. Bull. Plankton Soc. Japan 55 (2), 107-114.

van der Meeren, T., Næss, T., 1993. How does cod (*Gadus morhus*) cope with variability in feeding conditions during early larval stages? Mar. Biol. 116 (4), 637-647.

Yamaguchi, A., Watanabe, Y., Ishida, H., Harimoto, T., Maeda, M., Ishizaka, J., Ikeda,

494 T., Takahashi, M.M., 2005. Biomass and chemical composition of net-plankton
495 down to greater depth (0-5800 m) in the western North Pacific Ocean. Deep-Sea
496 Res. I 52 (2), 341-353.
497 Yamaguchi, A., Onishi, Y., Omata, A., Kawai, M., Kaneda, M., Ikeda, T., 2010.
498 Population structure, egg production and gut content pigment of large grazing
499 copepods during the spring phytoplankton bloom in the Oyashio region. Deep-Sea
500 Res. II 57 (17-18), 1679-1690.
501 Yamamura, O., 2004. Trophodynamics modeling of walleye Pollock (*Theragra*
502 *chalcogramma*) in the Doto area, northern Japan: model description and baseline
503 simulations. Fish. Oceanogr. 13 (S1), 138-154.
504 Yasuda, I., Okuda, K., Hirai, M., 1992. Evolution of a Kuroshio warm-core ring -
505 variability of the hydrographic structure. Deep-Sea Res. A 39 (S1), S131-S161.
506 Yokoi, Y., Yamaguchi, A., Ikeda, T., 2008. Regional and interannual changes in the
507 abundance, biomass and size structure of mesozooplankton in the western North
508 Pacific in early summer analysed using an optical plankton counter. Bull. Plankton
509 Soc. Japan 55 (1), 9-24.
510 Zhang, X., Roman, M., Sanford, A., Adolf, H., Lascara, C., Burgett, E., 2000. Can an
511 optical plankton counter produce reasonable estimate of zooplankton abundance
512 and biovolume in water with high detritus? J. Plankton Res. 22 (1), 137-150.
513

514 Figure legends

515 Fig. 1. Location of the Oyashio region in the western subarctic Pacific (a) and of
516 sampling station Site H in the Oyashio region (b).

517 Fig. 2. Relationship between the OPC-derived ESD and prosome length (PL) of
518 copepods (a) and between OPC-derived wet mass and directly measured wet
519 mass (b).

520 Fig. 3. Temporal changes in integrated mean temperature and salinity in the 0-150 m
521 water column in the Oyashio region (a). Values are means of 2002-2007.
522 Temporal changes in the T-S diagram of integrated mean values for the 0-150
523 m water column (b). Values in panel (b) indicate sigma-T (density).
524 Classification of water masses (Hanawa and Mitsudera, 1987) is also shown
525 in (b). O: Oyashio Water, SW: Surface-layer water and TW: Tsugaru Warm
526 Water.

527 Fig. 4. Temporal changes in zooplankton size composition derived from OPC
528 analysis: abundance in the 0-150 m (a) and 150-500 m (b) strata of the water
529 column and biomass in the 0-150 m (c) and 150-500 m (d) strata in the
530 Oyashio region.

531 Fig. 5. Temporal changes in biomass in the 0-150 m stratum (upper panels) and the
532 150-500 m stratum of the water column (lower panels) in the Oyashio region
533 for each ESD size class: <0.5 mm (a), 0.5-1.0 mm (b), 1.0-2.0 mm (c),
534 2.0-3.0 mm (d), 3.0-4.0 mm (e) and >4.0 mm (f), analysed by OPC
535 measurement.

536 Fig. 6. Temporal changes in abundance (upper panels) and biomass (lower panels)
537 and stage compositions of *Neocalanus cristatus* (a), *N. flemingeri* (b) and *N.*

538 *plumchrus* (c) in the Oyashio region. Note that the biomass was estimated
539 by multiplying individual mass by abundance (Ueda et al., 2008).
540 Fig. 7. Temporal changes in abundance (upper panels) and biomass (lower panels)
541 and stage compositions of *Eucalanus bungii* (a) and *Metridia pacifica* (b) in
542 the Oyashio region. Note that the biomass was estimated by multiplying
543 individual mass by abundance (Ueda et al., 2008).
544 Fig. 8. Temporal changes in the species composition of dominant copepods in terms
545 of zooplankton biomass for each size class (<0.5 [a], 0.5-1.0 [b], 1.0-2.0 [c],
546 2.0-3.0 [d], 3.0-4.0 mm [e] and Total [f]) in the 0-500 m water column of the
547 Oyashio region, derived from microscopic analysis (Figs. 5 and 6) and OPC
548 analysis (Fig. 4). Note that the biomass of "Others" is calculated as the
549 difference ([OPC derived mass] – [Microscopic derived copepod mass]).

Table 1

Click here to download Table: Table-1.ppt

Table 1. Zooplankton sampling dates at Site H in the Oyashio region, western subarctic Pacific during 2002-2007.

2002/2003		2004/2005		2006/2007	
Date	Day of year	Date	Day of year	Date	Day of year
18 May '02	139	7 Feb. '04	39	10 Mar. '06	70
6 June '02	158	9 Mar. '04	70	11 Mar. '06	71
12 July '02	194	13 Mar. '04	74	9 May '06	130
12 Aug. '02	225	15 Mar. '04	76	18 May '06	139
8 Oct. '02	282	9 May '04	131	23 May '06	144
17 Dec. '02	352	1 June '04	154	2 June '06	154
11 Feb. '03	42	11 June '04	164	29 July '06	181
11 Mar. '03	71	25 June '04	178	25 Oct. '06	299
10 May '03	131	21 Aug. '04	235	26 Oct. '06	300
20 May '03	141	4 Sep. '04	249	27 Oct. '06	301
3 June '03	155	5 Sep. '04	250	14 Dec. '06	349
14 June '03	166	14 Dec. '04	349	15 Dec. '06	350
27 June '03	179	15 Dec. '04	350	8 May '07	129
22 Aug. '03	235	19 Mar. '05	79	18 May '07	139
4 Oct. '03	278	10 May '05	131	1 July '07	183
16 Dec. '03	351	21 May '05	142	25 Aug. '07	238
		29 May '05	150	10 Dec. '07	345
		3 June '05	155	11 Dec. '07	346
		13 June '05	165		
		27 June '05	179		
		22 Aug. '05	235		
		14 Dec. '05	349		

Table 2

Click here to download Table: Table-2.pdf

Table 2. Equivalent spherical diameter (ESD) size class of each copepodid stage of the dominant calanoid copepods in the Oyashio region. Mean ESD values are shown with ± 1 sd in the parentheses. All the measurements were done for 30 individuals of each stage. Note that the sex separation was not done for *Neocalanus* spp. because of the low abundance. *: C6 of *N. cristatus* was estimated from the prosome length ratio between C6 and C5 reported by Kobari and Ikeda (1999).

Size class (ESD: mm)	*Neocalanus cristatus*		*Neocalanus flemingeri*		*Neocalanus plumchrus*		*Eucalanus bungii*		*Metridia pacifica*	
< 0.5			C1	(0.409 ± 0.040)	C1	(0.417 ± 0.06)			C1	(0.411 ± 0.088)
									C2	(0.451 ± 0.044)
									C3	(0.490 ± 0.074)
0.5-1.0	C1	(0.509 ± 0.059)	C2	(0.667 ± 0.124)	C2	(0.569 ± 0.102)	C1	(0.635 ± 0.069)	C4F	(0.586 ± 0.071)
	C2	(0.823 ± 0.101)	C3	(0.846 ± 0.098)	C3	(0.833 ± 0.082)	C2	(0.793 ± 0.116)	C4M	(0.584 ± 0.089)
									C5F	(0.868 ± 0.100)
									C5M	(0.774 ± 0.088)
									C6M	(0.814 ± 0.132)
1.0-2.0	C3	(1.504 ± 0.225)	C4	(1.324 ± 0.191)	C4	(1.76 ± 0.140)	C3	(1.016 ± 0.102)	C6F	(1.489 ± 0.175)
							C4F	(1.447 ± 0.182)		
							C4M	(1.483 ± 0.162)		
							C5M	(1.916 ± 0.180)		
2.0-3.0	C4	(2.399 ± 0.456)	C5	(2.013 ± 0.255)	C5	(2.109 ± 0.292)	C5F	(2.031 ± 0.285)		
			C6	(2.097 ± 0.591)	C6	(2.141 ± 0.079)	C6F	(2.728 ± 0.416)		
							C6M	(2.303 ± 0.199)		
3.0-4.0	C5	(3.643 ± 0.368)								
	C6	3.750*								

Figure
Click here to download Figure: Fig-1.ppt

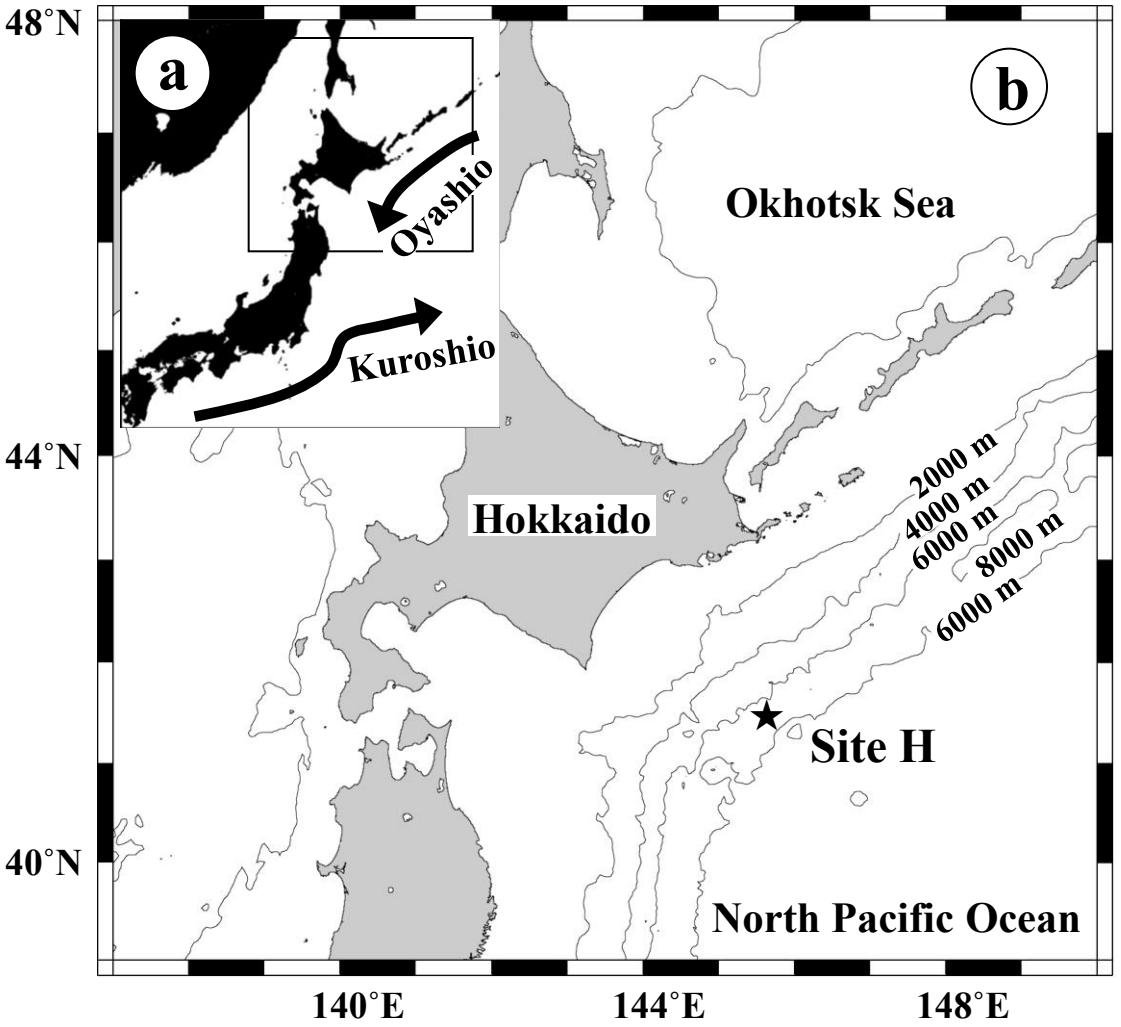

Fig. 1 (Yamaguchi et al.)

Figure
Click here to download Figure: Fig-2.ppt

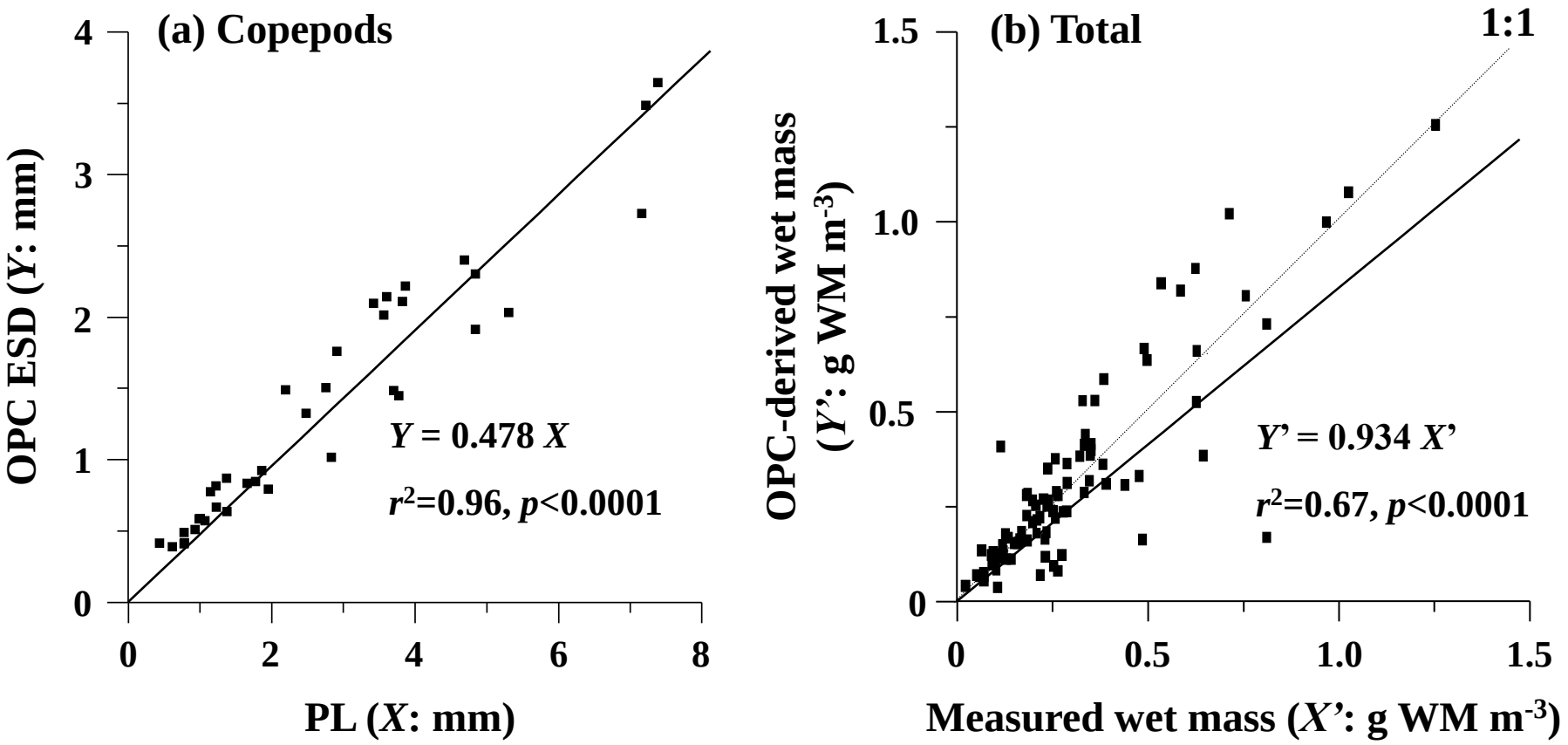

Fig. 2 (Yamaguchi et al.)

Figure
Click here to download Figure: Fig-3.ppt

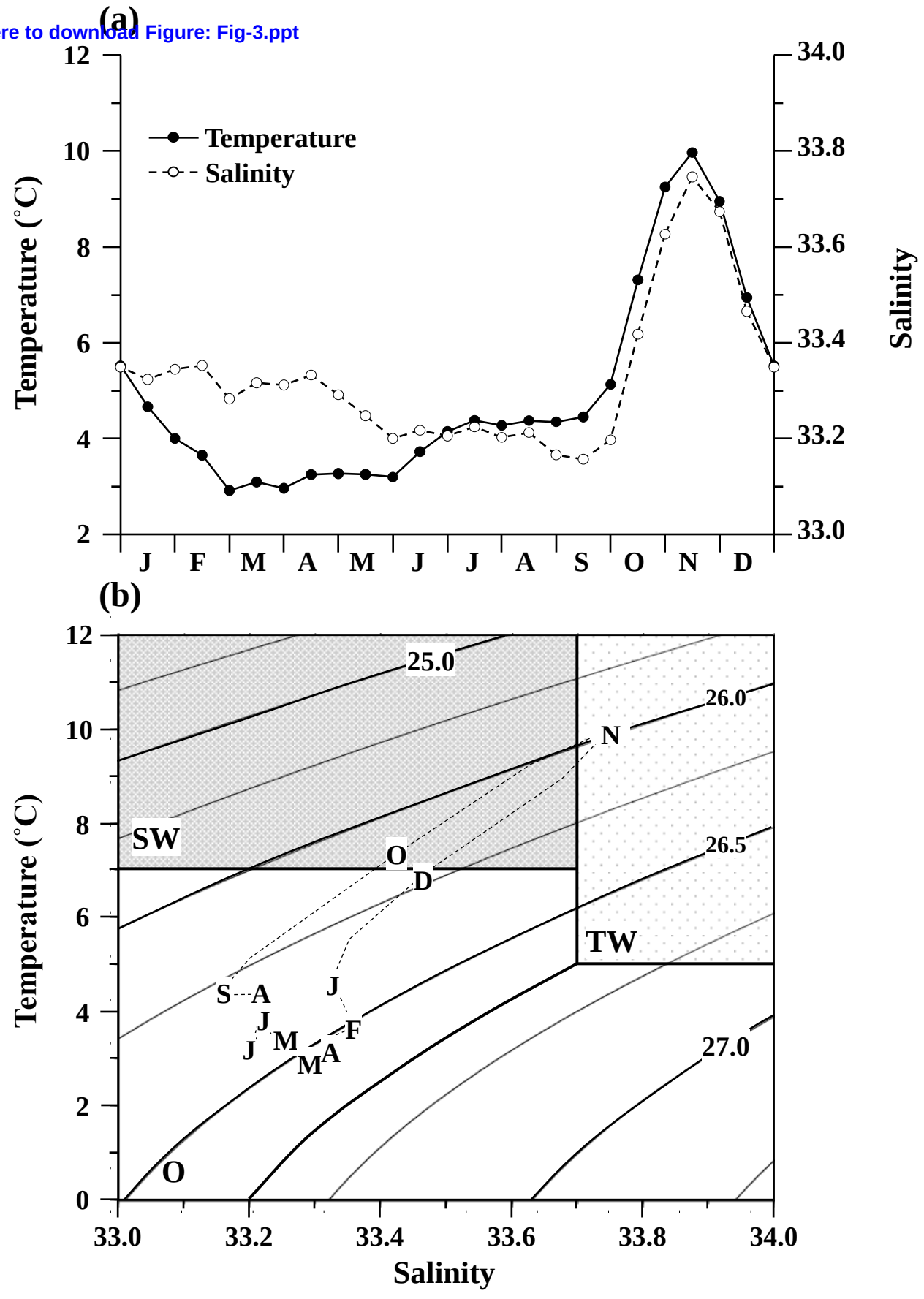

Fig. 3 (Yamaguchi et al.)

Figure
Click here to download Figure: Fig-4.ppt

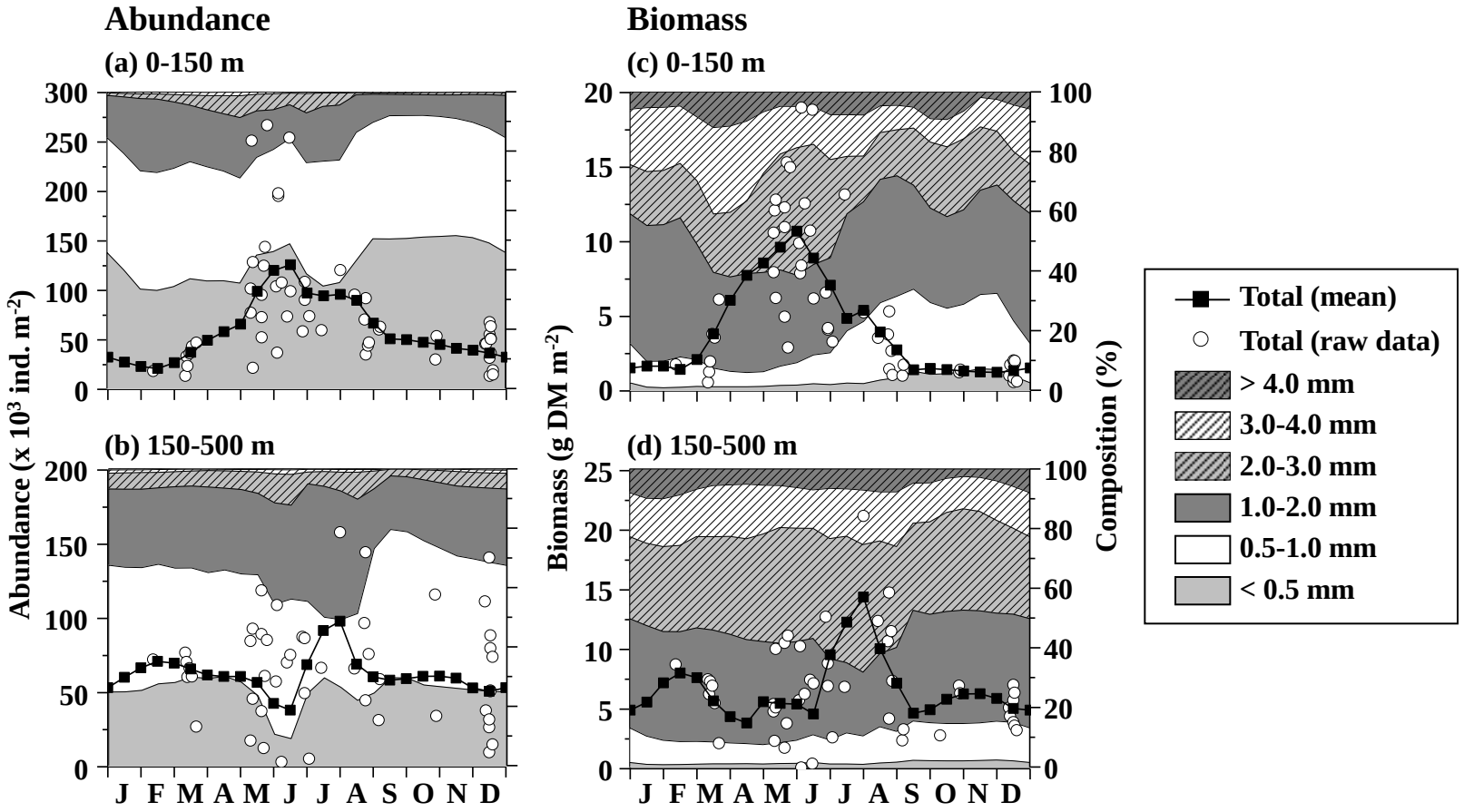

Fig. 4 (Yamaguchi et al.)

Figure
Click here to download Figure: Fig-5.ppt

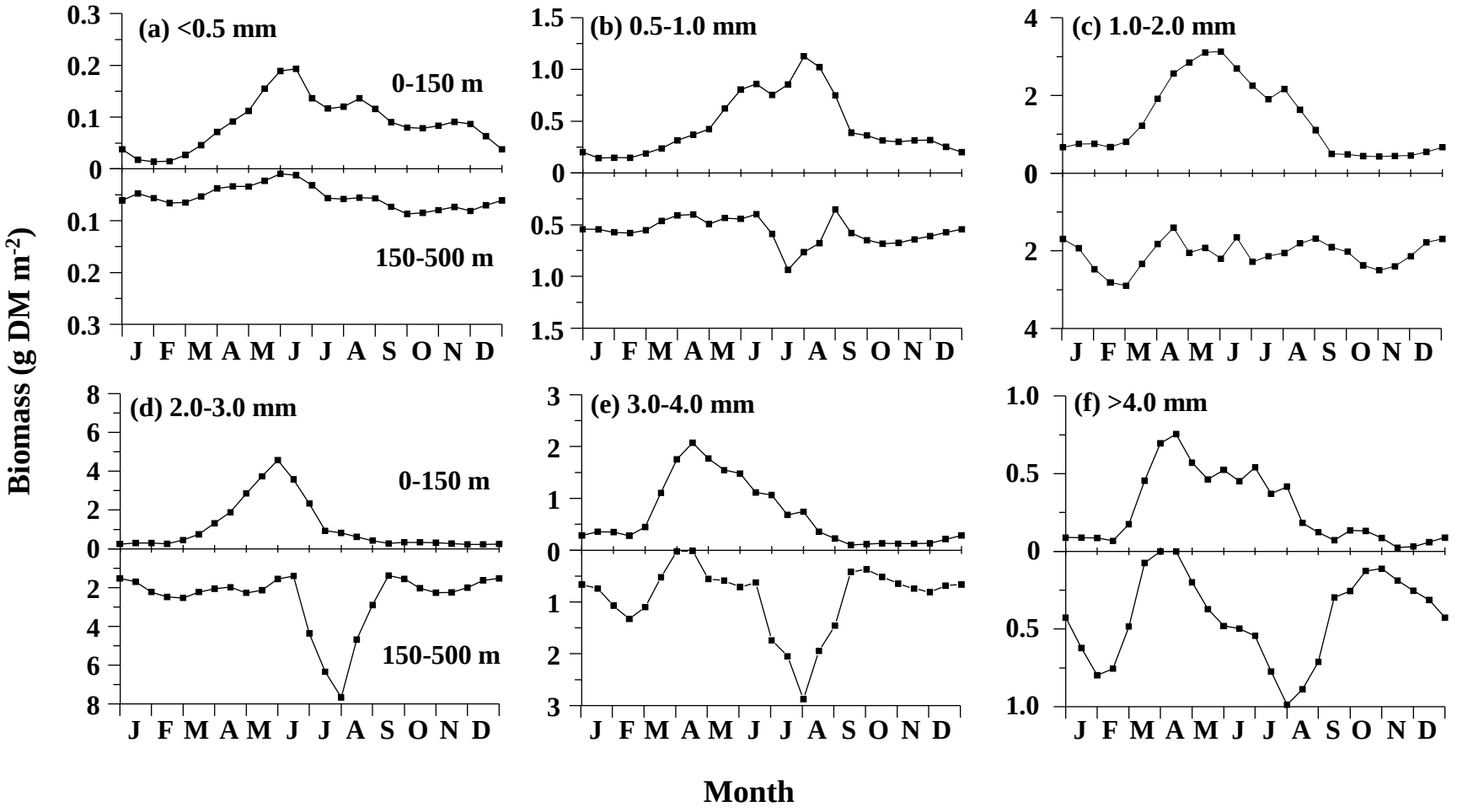

Fig. 5 (Yamaguchi et al.)

Figure

Click here to download Figure: Fig-6.ppt

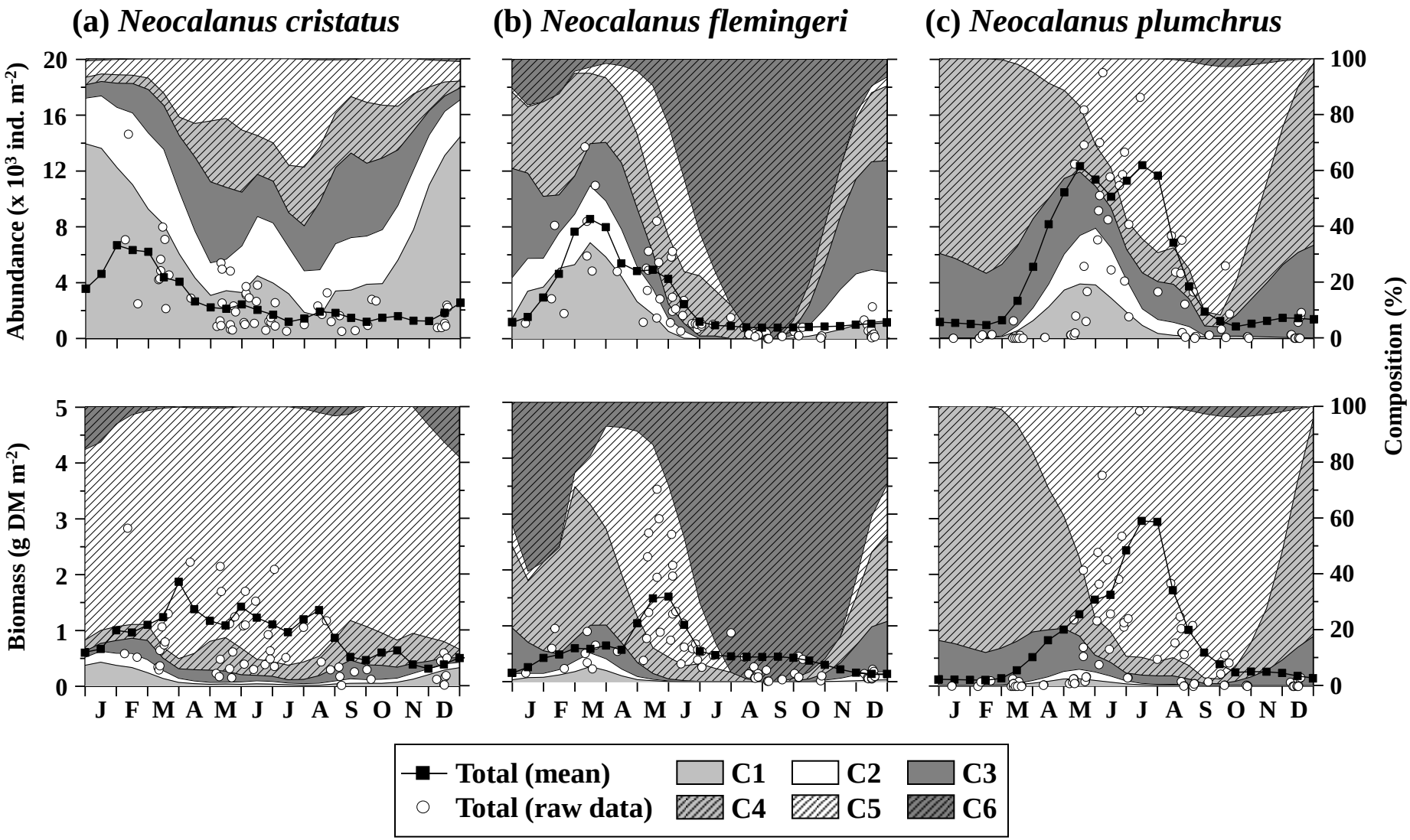

Fig. 6 (Yamaguchi et al.)

Figure
Click here to download Figure: Fig-7.ppt

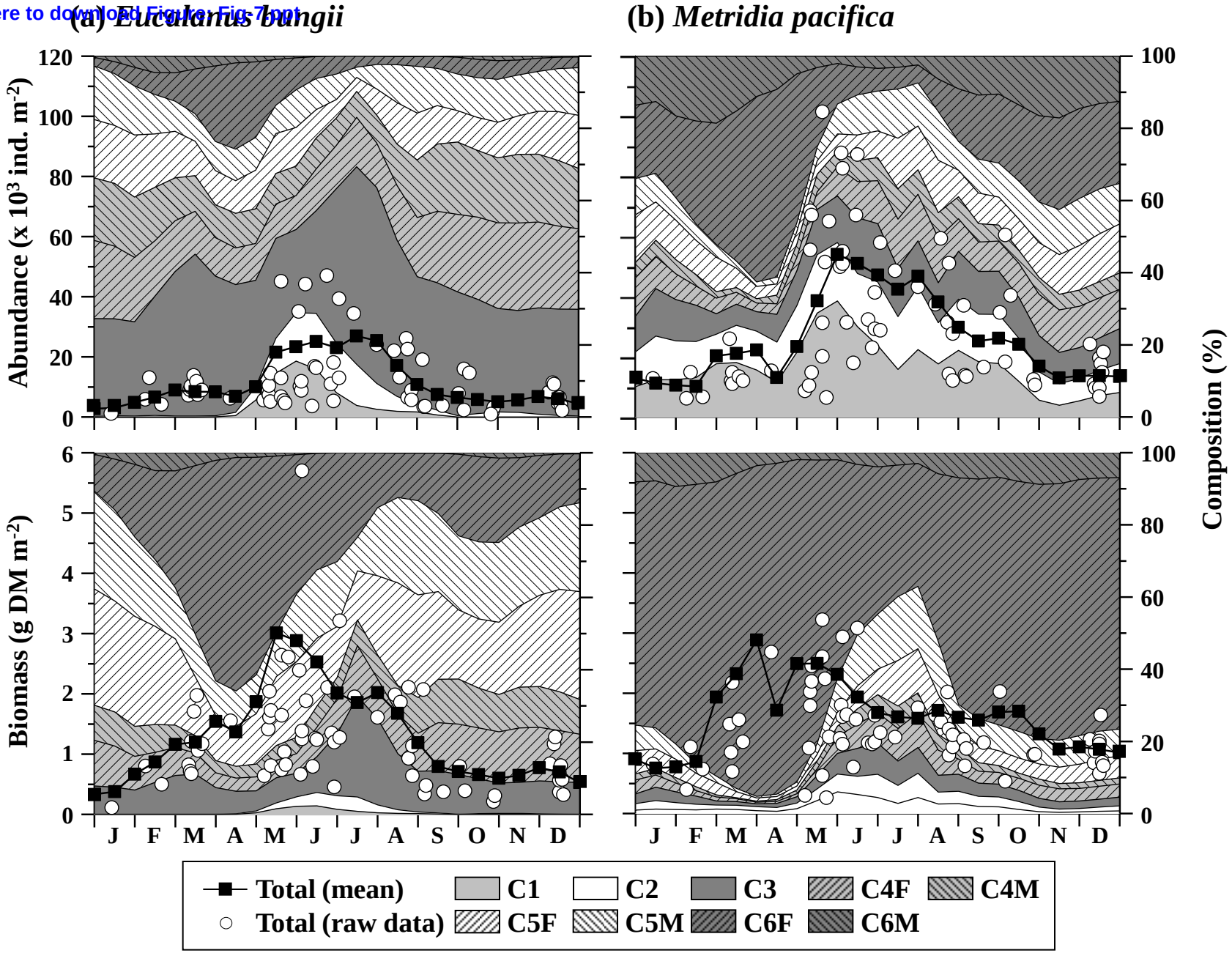

Fig. 7 (Yamaguchi et al.)

Figure
Click here to download Figure: Fig-8.ppt

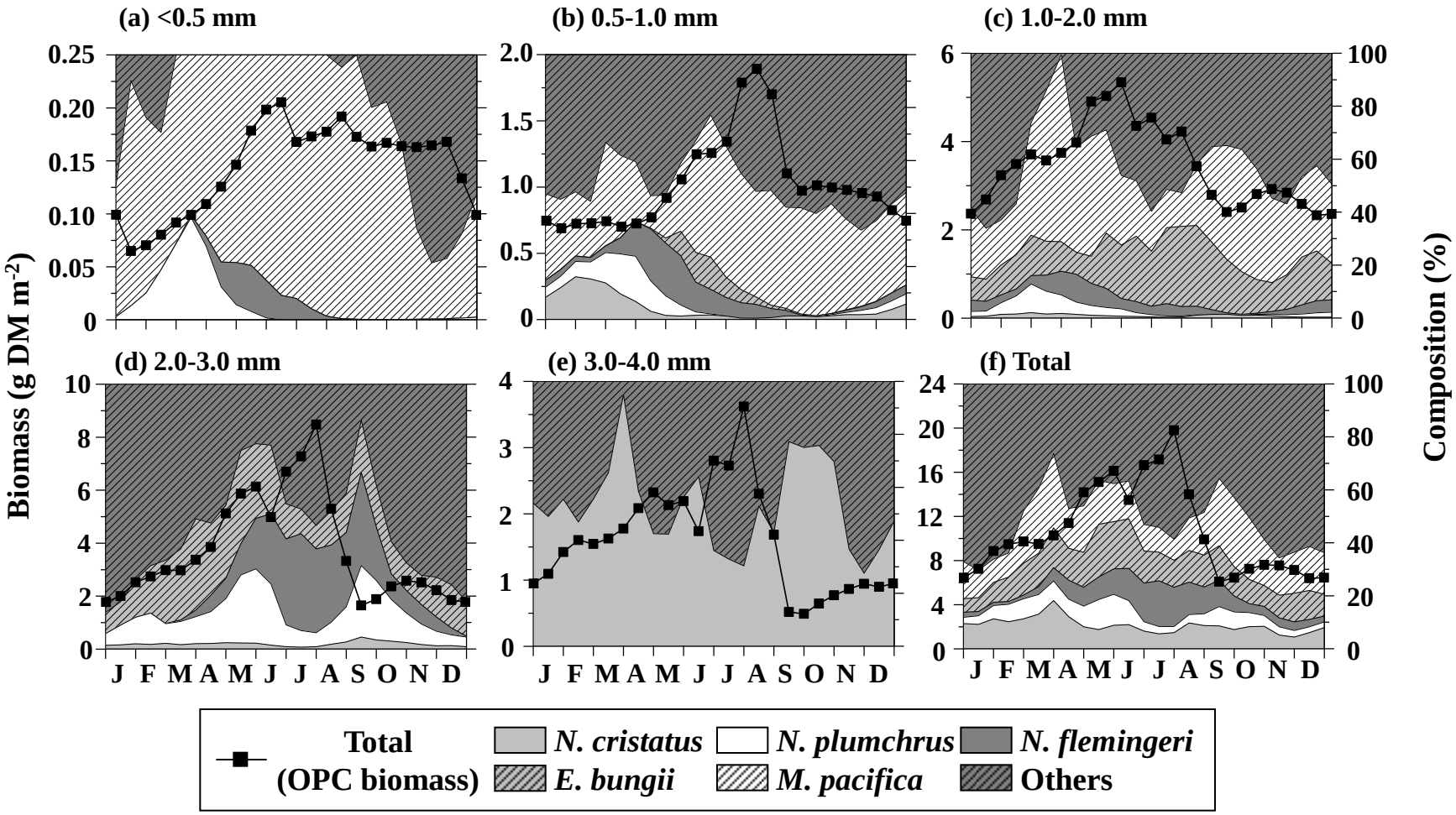

Fig. 8 (Yamaguchi et al.)